Electrochimica Acta 58 (2011) 209–214

Contents lists available at SciVerse ScienceDirect

Electrochimica Acta

journal homepage: www.elsevier.com/locate/electacta

Sensitive and selective nonenzymatic glucose detection using functional NiO–Pt hybrid nanofibers

Yu Ding[a], Yixin Liu[a], Lichun Zhang[b], Ying Wang[a], Michael Bellagamba[a], Joseph Parisi[a], Chang Ming Li[c], Yu Lei[a,*]

[a] Department of Chemical, Materials and Biomolecular Engineering, University of Connecticut, Storrs, CT 06269-3222, USA
[b] Institute of Material Science, University of Connecticut, Storrs, CT 06269-3222, USA
[c] School of Chemical and Biomedical Engineering, Nanyang Technological University, Singapore 637457, Singapore

ARTICLE INFO

Article history:
Received 16 June 2011
Received in revised form 29 August 2011
Accepted 14 September 2011
Available online 24 September 2011

Keywords:
NiO–Pt nanofibers
Glucose sensor
Electrospinning
Nonenzymatic

ABSTRACT

By calcining electrospun $Ni(NO_3)_2$–H_2PtCl_6–PVP composite nanofibers, Pt-doped NiO nanofibers have been successfully fabricated. Their morphologies were characterized using scanning electron microscopy and transmission electron microscopy, and structures were analyzed by X-ray diffraction. Tiny Pt nanoparticles (<10 nm) were dispersed in NiO matrix and the whole nanofiber displayed a rough surface and porous structure. The as-prepared hybrid nanofibers were employed for nonenzymatic glucose detection in alkaline electrolyte and showed greatly improved electrocatalytic activity compared to those obtained with pure NiO nanofibers and Pt nanofibers, with higher sensitivity (180.80 $\mu A\,mM^{-1}\,cm^{-2}$), lower detection limit (313 nM), and good linear range (up to 3.67 mM). These results suggest that electrospun NiO–Pt hybrid nanofibers are a promising nanomaterial for design and fabrication of electrochemical devices for glucose detection.

1. Introduction

In recent years, considerable attention has been paid to develop stable and sensitive enzyme-free electrodes to replace the enzyme (glucose oxidase or glucose dehydrogenase) based glucose sensors which usually suffer from stability problems due to the intrinsic features of proteins. Precious metals such as Pt and Au have been extensively studied in the construction of nonenzymatic electrochemical glucose sensors [1,2]. However, conventional Pt and Au electrodes are easily poisoned by the adsorbed intermediates and chloride, leading to low sensitivity. In addition, glucose detection at these electrodes is easily interfered by other electroactive compounds such as ascorbic acid (AA) and uric acid (UA) [3]. Varieties of nanostructured Pt has been synthesized to enhance the sensing performance, such as mesoporous Pt [4], highly ordered Pt-nanotubes arrays [5] and three dimensional ordered macroporous Pt [6]. It has been reported that sensitivity, selectivity and anti-fouling property may be improved by increasing the ratio of nanoscopic surface area to the geometric surface area (roughness factor) [4]. On the other hand, several Pt composites have also been investigated to address the poisoning issue and improve sensitivity, including Pt nanoparticles supported on carbon nanotubes [1], nanoporous Pt–Pb alloy networks [7], Pt–Pb alloy nanoparticles deposited on carbon nanotubes [8] and Pt–WO_3 composite wire [9]. Earlier studies also indicate the modification of Pt surfaces by other metals such as Tl, Bi, and Pb may alter the adsorption and oxidation route, leading to improved electrocatalytic activity towards glucose oxidation [7].

In this work, we fabricated a novel hybrid nanofiber consisting of Pt and NiO by the facile electrospinning technique followed by calcination. Electrospinning is a relatively simple and versatile method for fabricating nanofibers, which is originally applied to pure organic polymers [10]. Recently this technique has been extended to produce metal oxide or noble metal nanofibers by calcination of polymer composite nanofibers containing the corresponding metal salts. A series of metal oxide nanofibers, such as CuO [3,11], ZnO [12], Co_3O_4 [13,14], NiO [15] and TiO_2 [10,16], and noble metal nanofibers such as Ag [17], Au [18] and Pt [19] have been developed following this two-step procedure. NiO has been reported as a good catalyst for glucose electrooxidation in alkaline medium, which has negligible intermediates- or chloride-associated poisoning issue [3,15]. To prepare Pt-doped NiO nanofibers, $Ni(NO_3)_2$ and H_2PtCl_6 were co-dissolved in poly(vinyl pyrrolidone) (PVP) solution and electrospun to generate precursory composite nanofibers. After calcination in air at 500 °C for 3 h, the polymer matrix was completely degraded and $Ni(NO_3)_2$ was decomposed to NiO while H_2PtCl_6 was converted to Pt, since noble metal tends to stay in a zero oxidation state. Pt nanoparticles were well distributed in/on

* Corresponding author. Tel.: +1 860 486 4554; fax: +1 860 486 2959.
E-mail address: ylei@engr.uconn.edu (Y. Lei).

0013-4686/$ – see front matter © 2011 Elsevier Ltd. All rights reserved.
doi:10.1016/j.electacta.2011.09.039

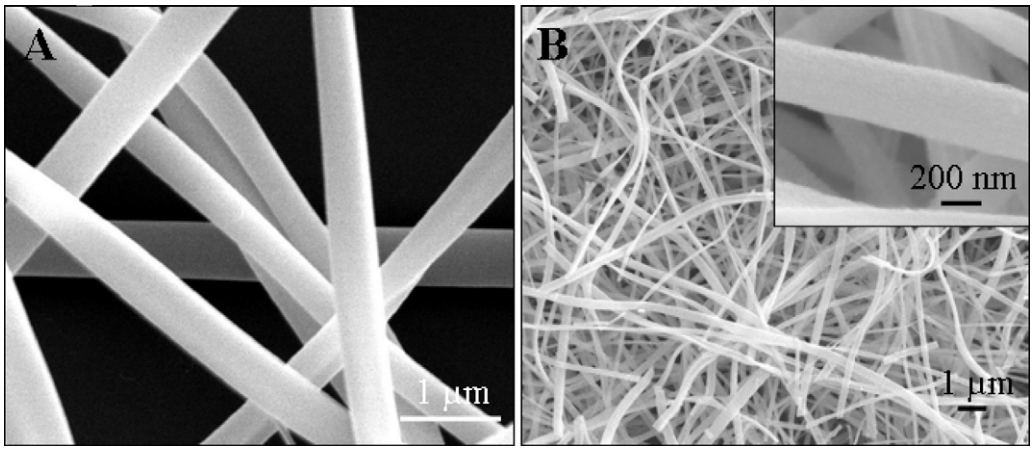

Fig. 1. SEM images of (A) $Ni(NO_3)_2$–H_2PtCl_6–PVP nanofibers electrospun from PVP sol–gel in ethanol–water containing $Ni(NO_3)_2$ and H_2PtCl_6; (B) NiO–Pt nanofibers; inset shows a SEM image with higher magnification.

the NiO nanofibers. The as-prepared hybrid nanofibers were then employed for glucose detection in alkaline electrolyte and the combination of NiO and Pt was expected to offer a synergistic effect between individual components: on one hand, the NiO matrix can prevent the adsorption of poisoning species on the Pt surfaces; on the other hand, the Pt dopants may provide more opportunities for electron transfer due to its good electron conductivity.

2. Experimental

2.1. Reagents

Nickel nitrate hexahydrate ($Ni(NO_3)_2{\cdot}6H_2O$), hydrogen hexachloroplatinate(IV) hexahydrate ($H_2PtCl_6{\cdot}6H_2O$) and D-(+)-glucose were purchased from Acros Organics. Sodium hydroxide (NaOH) was supplied by Fisher Scientific. Poly(vinyl pyrrolidone) (PVP, MW = 1,300,000) and Nafion® perfluorinated resin solution (20 wt% in lower aliphatic alcohols and water, containing 34% water) were obtained from Sigma–Aldrich. All aqueous solutions were prepared with deionized water (18.2 MΩ cm) generated by a Barnstead water system.

2.2. Preparation of NiO–Pt nanofibers modified electrode

0.4 g $Ni(NO_3)_2{\cdot}6H_2O$ and 0.1 g $H_2PtCl_6{\cdot}6H_2O$ were dissolved in 1.6 g water and then mixed with a 2.8 g solution consisting of 0.4 g PVP and 2.4 g ethanol. The $Ni(NO_3)_2$–H_2PtCl_6–PVP composite nanofibers were prepared using a 23-gauge needle with a flow rate of 0.3 mL/h at an applied voltage of 20 kV over a gap distance of 15 cm and were collected on aluminum foil. The precursor was then calcined under air atmosphere at 500 °C for 3 h in order to remove the polymer matrix and generate NiO–Pt nanofibers. In order to prepare stable H_2PtCl_6–PVP sol–gel and produce Pt nanofibers with good morphology, 0.3864 g $H_2PtCl_6{\cdot}6H_2O$ and 0.3864 g PVP were dissolved in 4.5 mL DMF/H_2O (3 mL DMF plus 0.5 mL H_2O). To prepare 5 mg/mL NiO–Pt nanofibers suspension, 5 mg NiO–Pt nanofibers was first suspended in 1 mL ethanol and sonicated for 1 h, and then a 5 μL suspension was dropped onto the surface of glassy carbon electrode (GCE). After drying in air, an aliquot of 5 μL Nafion solution (1 wt% in ethanol) was cast on the layer of NiO–Pt nanofibers in order to entrap NiO–Pt nanofibers. The as-prepared electrode (denoted as NiO–Pt NFs/GCE) was immersed in water for 1 h to wet the Nafion layer thoroughly before use. Similar procedure was also applied to prepare NiO or Pt nanofibers modified GCEs (NiO NFs/GCE and Pt NFs/GCE).

2.3. Apparatus and electrochemical measurements

A JEOL 6335F field-emission scanning electron microscope (SEM) was employed to examine the morphology and the size of the as-electrospun nanofibers before and after calcination. More detailed morphology and selected area electron diffraction (SAED) patterns were studied using a Tecnai T12 transmission electron microscope (TEM) operated at 120 kV. High resolution TEM images were obtained at a JEOL 2010 FasTEM. XRD patterns of the as-prepared samples were obtained with an Oxford diffraction Xcalibur™ PX Ultra with ONYX detector. Cyclic voltammetry (CV) measurements were performed on a Model CHI 601C Electrochemical Workstation (CH Instruments, USA). All electrochemical experiments were conducted using a three-electrode electrochemical cell (a working volume of 5 mL) with a working electrode, an Ag/AgCl (3 M KCl) reference electrode, and a platinum wire counter electrode. For amperometric detection, all measurements were performed by applying an appropriate potential to the working electrode and allowing the transient background current to decay to a steady-state value, before the addition of the analyte. A stirred solution was employed to provide convective transport.

3. Results and discussion

3.1. Characterization of the nanofibers before and after calcination

Fig. 1A shows the SEM image of $Ni(NO_3)_2$–H_2PtCl_6–PVP composite nanofibers electrospun from PVP sol–gel containing $Ni(NO_3)_2$ and H_2PtCl_6 using ethanol–water as the solvent. Each nanofiber was uniform with an average diameter of 464 ± 27 nm. The formation of this type of quasi-one dimensional structure may be attributed to the high concentration of metal salts contained in sol–gel, which may lead to the incomplete drying of the inner part of ejected fibers before reaching the collector; while the skin on the surface easily became dry due to the rapid evaporation of solvent. The collapse of the skin caused the fibers to have a flat shape [20,21]. The SEM morphology of the calcined sample is presented in Fig. 1B, indicating the continuous and flat nanofiber structure is still kept, while the surfaces become rough (clearly shown in the inset) and the average diameter decreases to 214 ± 77 nm.

The detailed morphology of the as-prepared NiO–Pt nanofibers was further characterized by TEM. Fig. 2A reveals that the nanofibers consist of numerous nanoparticles which possess large surface area and minimize transport hindrance for subsequent catalytic reactions [3]. The rings displayed in selected area electron

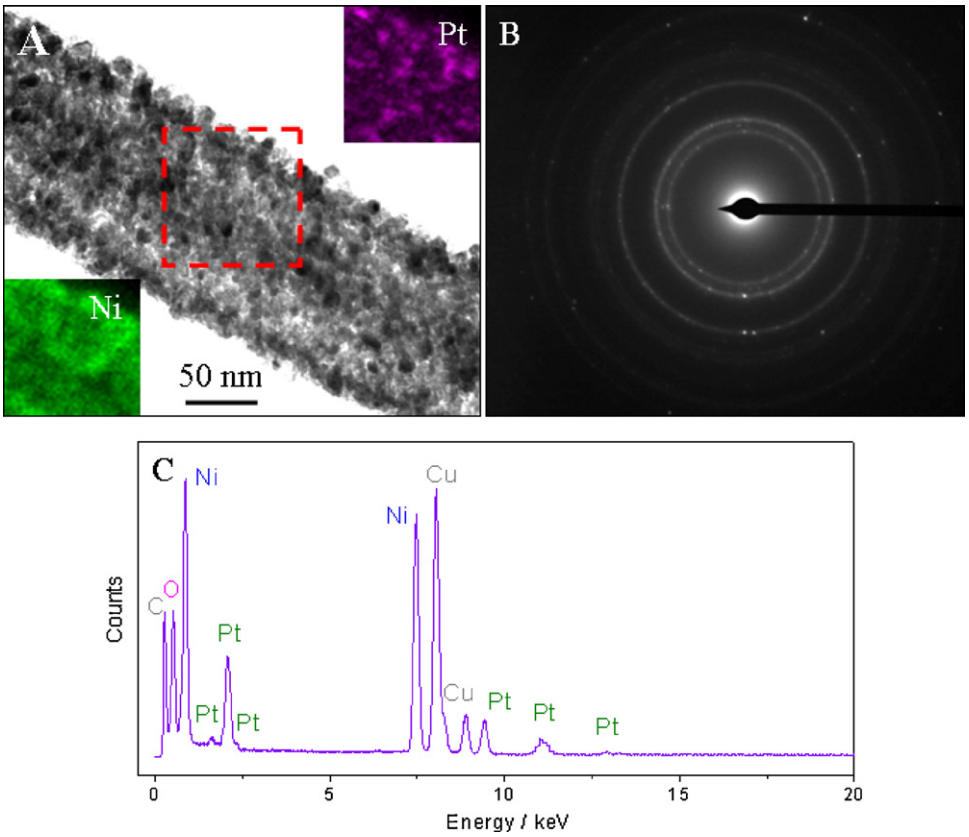

Fig. 2. (A) TEM image of single NiO–Pt nanofiber; insets indicate the EDX mapping of Ni and Pt element, respectively. (B) SAED pattern of the NiO–Pt nanofibers. (C) EDX analysis of the NiO–Pt nanofibers; Cu and C peaks come from the TEM grid.

diffraction (SAED) pattern indicate the polycrystalline structure of the hybrid nanofibers. X-ray energy dispersive spectroscopy (EDX) was carried to analyze the compositions of the calcined sample and the results shown in Fig. 2C imply the presence of Ni, O and Pt (Cu and C peaks are attributed to the TEM grid). The distribution of NiO and Pt was further characterized by EDX mapping. The two insets in Fig. 2A display the heterogeneous and discontinuous distribution of Pt, while the distribution of NiO as the matrix is relatively uniform and continuous. It is notable that the Pt is dispersed as tiny dots with very small particle size (<10 nm). A high resolution TEM (HRTEM) lattice image of the NiO–Pt nanofiber is shown in Fig. 3, indicating the doping of tiny Pt crystallites in the NiO matrix.

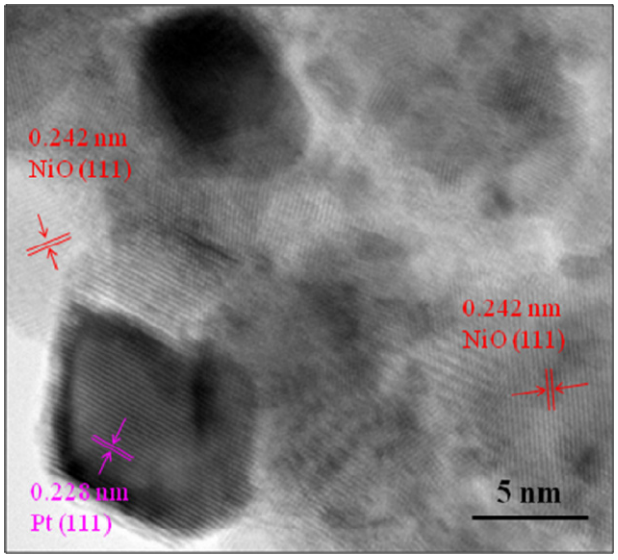

Fig. 3. HRTEM lattice image of NiO–Pt nanofiber.

The electrospinning cannot smoothly generate nanofibers when the PVP sol–gel only containing H_2PtCl_6 was prepared in ethanol/H_2O as the solvent. Therefore we used a DMF/H_2O system as the solvent to dissolve PVP and H_2PtCl_6. Uniformly distributed, continuous and smooth H_2PtCl_6–PVP composite nanofibers with an average diameter of 190 ± 19 nm were fabricated (Fig. 4A). After calcination, the size of nanofibers was greatly shrunk to 39 ± 6 nm (Fig. 4B) and the calcined Pt nanofibers consisted of elongated Pt nanoparticles and displayed a necklace-like structure (Fig. 4C).

In order to confirm the structure and composition of both NiO–Pt nanofibers and Pt nanofibers, X-ray diffraction (XRD) was performed. As shown in Fig. 5, the XRD spectrum of NiO–Pt composites matches the combination of the spectra of NiO (JCPDS 04-0835) and Pt (JCPDS 04-0802). The formation of face-centered cubic crystalline NiO is revealed by the diffraction peaks at 2θ values of 37.28°, 43.30°, 62.92° corresponding to (1 1 1), (2 0 0) and (2 2 0) main crystal planes, respectively; while the diffraction peaks at 2θ values of 39.76°, 46.24°, 67.45°, which correspond to (1 1 1), (2 0 0), and (2 2 0) crystal planes respectively, indicates the formation of cubic crystalline Pt.

3.2. *Electrochemistry behavior of NiO–Pt NFs, NiO NFs, and Pt NFs modified GCEs*

Electrooxidation of glucose at Pt nanofibers in 0.1 M NaOH (pH = 13) was examined in the range of −0.3 V to 0.7 V. The lowest applied potential was set at −0.3 V in order to prevent the reduction of dissolved oxygen in the solution. As shown in Fig. 6A, a current increase (or a shoulder peak) at ca. −0.25 V is observed

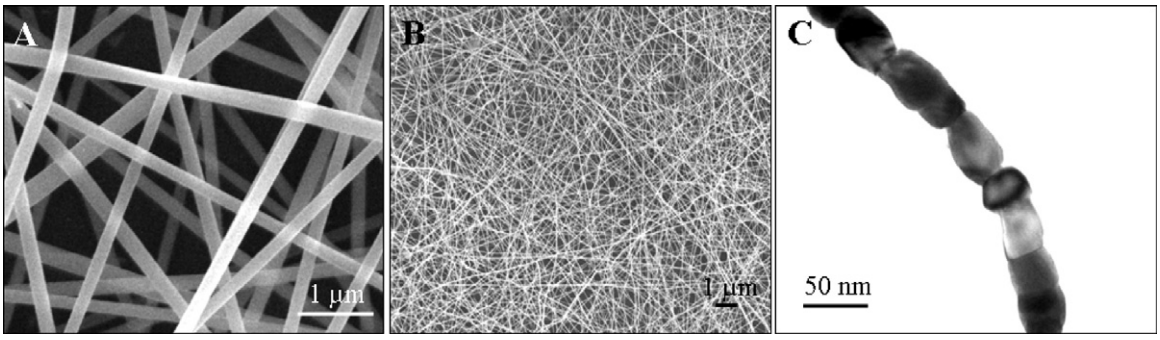

Fig. 4. SEM images of (A) H_2PtCl_6–PVP nanofibers electrospun from PVP sol–gel in DMF/H_2O containing H_2PtCl_6; (B) Pt nanofibers. (C) TEM image of a single Pt nanofiber.

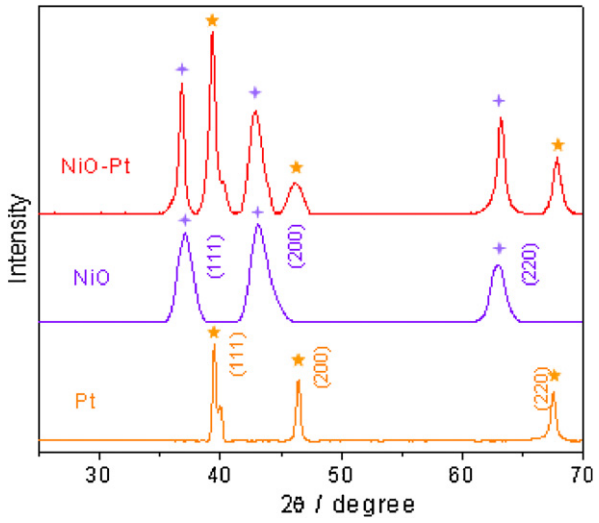

Fig. 5. XRD patterns for NiO–Pt, NiO and Pt nanofibers.

in the presence of glucose, which may be attributed to the oxidation of adsorbed intermediates by Pt–OH species [22,23]. This oxidation process eliminated the adsorbed intermediates derived from the electrochemical adsorption of glucose at lower potential and thus released active catalytic sites for the direct oxidization of glucose, leading to another oxidation peak at ca. +0.126 V. Further increase of the applied potential led to the formation of platinum oxide, which sacrificed the active sites and thus decreased the oxidation current [1]. As a comparison, the CV of the NiO–Pt NFs/GCE (Fig. 6B, trace c) was quite different from that of the Pt NFs/GCE (Fig. 6A) but similar with that of the NiO NFs/GCE (Fig. 6B, trace a), both CVs show a pair of well-defined redox peaks assigned to Ni^{2+}/Ni^{3+} redox couple ($NiO + OH^- - e^- \rightarrow NiO(OH)$). When using NiO–Pt hybrid nanofibers as the sensing material, the oxidation current upon the addition of glucose obtained at potentials less than +0.3 V was insignificant; while at the potentials above +0.3 V, the response was rapidly increased with the applied potential, showing similar trend with that obtained at the NiO NFs/GCE, but with much higher current signal, which may be attributed to the excellent electron transfer properties of the doped Pt.

In order to determine the optimum applied potential for real-time detection, hydrodynamic voltammogram (HDV) was further conducted by measuring the amperometric responses to 200 μM glucose at different applied potentials from 0 V to 0.6 V. As expected, the HDV of NiO–Pt showed similar shape with that of NiO, but current responses were greatly enhanced (Fig. 7A). Oxidation current of glucose can also be obtained in the potential range from 0.1 V to 0.3 V, illustrating the function of Pt in decreasing the onset potential and improving the electrocatalytic sensitivity. Since the response to glucose increased with the applied potential and too high potential may also favor the oxidation of interference, +0.6 V was adopted as the optimal potential for real-time detection.

Fig. 7B compares the amperometric responses of the NiO–Pt, NiO and Pt nanofibers modified electrodes at +0.6 V with successive additions of glucose. In these three cases, current signals all increase rapidly after each addition of glucose to the stirred solution, achieving 95% steady-state current within 4.1 s (NiO–Pt), 5.2 s (NiO) and 5.7 s (Pt), respectively. Their sensitivity, detection limit (S/N = 3), and linear range (obtained from calibration curves shown in Fig. 7C) are listed and compared in Table 1. The sensitivity of the NiO–Pt NFs/GCE is 5.5-fold greater than that obtained at the NiO NFs/GCE and 28.8-fold of the Pt NFs/GCE. Moreover, the linear range and the limit of detection have also been greatly improved. The analytical parameters of the NiO–Pt NFs/GCE for nonenzymatic

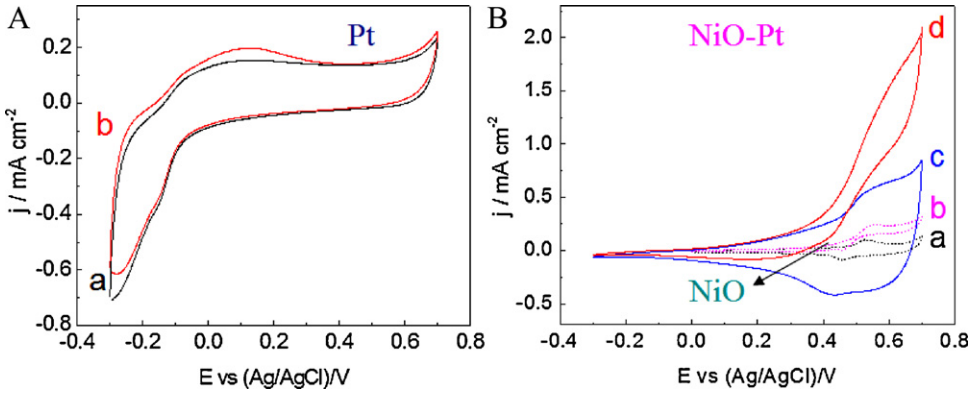

Fig. 6. (A) CVs of Pt NFs/GCE in the absence (a) and presence of 4 mM glucose (b) in 0.1 M NaOH. (B) CVs of NiO NFs/GCE (a and b) and NiO–Pt NFs/GCE (c and d) in the absence (a and c) and presence of 4 mM glucose (b and d) in 0.1 M NaOH. The scan rate is 100 mV/s.

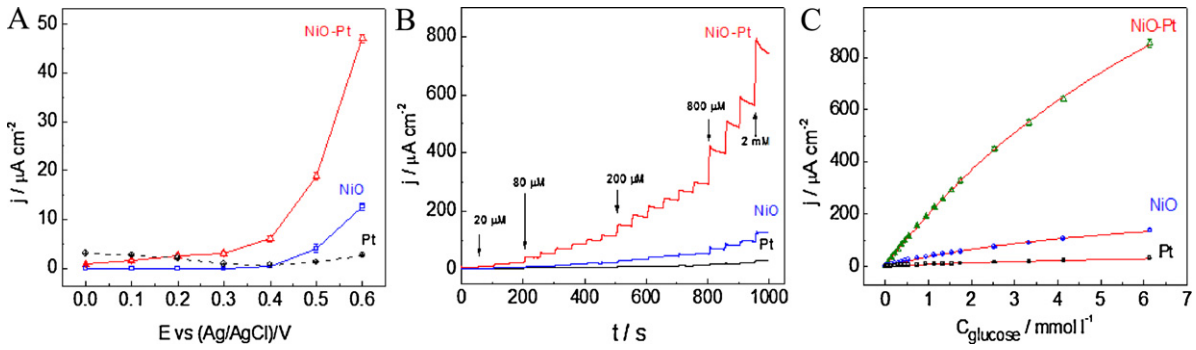

Fig. 7. (A) Hydrodynamic voltammograms of 200 μM glucose at the NiO–Pt, NiO and Pt nanofibers modified electrodes in 0.1 M NaOH solution with a stirring rate of 300 rpm. (B) Amperometric response of NiO–Pt NFs/GCE, NiO NFs/GCE and Pt NFs/GCE to successive additions of glucose to 0.1 M NaOH solution with a stirring rate of 300 rpm at an applied potential of +0.6 V, respectively. (C) The calibration curves with corresponding Langmuir fitting curves.

glucose detection are among the best reported values in the literature [4,24–29]. In order to apply the developed sensor for real samples, where commonly found glucose concentrations are in the range of 4–7 mM, Langmuir isothermal theory is used to fit the calibration curves because electrochemical oxidation of glucose on the electrode is a surface catalytic reaction, following Langmuir isothermal theory [14]. The corresponding fitting equations for NiO–Pt NFs/GCE, NiO/GCE, and Pt NFs/GCE are presented as follows:

For NiO–Pt NFs/GCE ($R^2 = 0.99973$),

$$I = \frac{15.48C_{\text{glucose}}}{1 + 0.09548C_{\text{glucose}}}$$

For NiO NFs/GCE ($R^2 = 0.99646$),

$$I = \frac{2.970C_{\text{glucose}}}{1 + 0.1486C_{\text{glucose}}}$$

For Pt NFs/GCE ($R^2 = 0.9981$),

$$I = \frac{0.5658C_{\text{glucose}}}{1 + 0.1114C_{\text{glucose}}}$$

In this way, the developed NiO–Pt NFs/GCE can be applied to very broad range of glucose concentration.

To evaluate the selectivity of the proposed biosensor, two interfering compounds, ascorbic acid (AA) and uric acid (UA), which usually coexist with glucose in real samples are examined. Taking into account the concentrations of glucose (4–7 mM), AA (0.125 mM) and UA (0.33 mM) in human blood [22,30], amperometric responses to 4 mM glucose and the same amount of glucose with 0.125 mM AA or 0.33 mM UA were compared. As shown in Fig. 8, the presence of 0.125 mM AA and 0.33 mM UA induces 36.6% and 38.7% current increase at Pt NFs/GCE, respectively; while such current increase drops dramatically at NiO–Pt NFs/GCE (1.42% for AA and 3.62% for UA). In order to elaborate the role of Nafion and NiO in such good selectivity, further selectivity study was conducted using high concentration of UA and AA (1 mM UA and 1 mM AA) as well as 4 mM glucose and the result is presented in Fig. S1. One can see

Table 1
Analytical characteristics of NiO–Pt, NiO and Pt NFs/GCE at +0.6 V vs. Ag/AgCl.

	NiO–Pt NFs/GCE	NiO NFs/GCE	Pt NFs/GCE
Linear range up to/mmol l^{-1}	3.67	1.94	2.63
Detection limit/μmol l^{-1}	0.313	1.28	4.02
Sensitivity/μA (mmol l^{-1})$^{-1}$ cm^{-2}	180.80	32.91	6.27

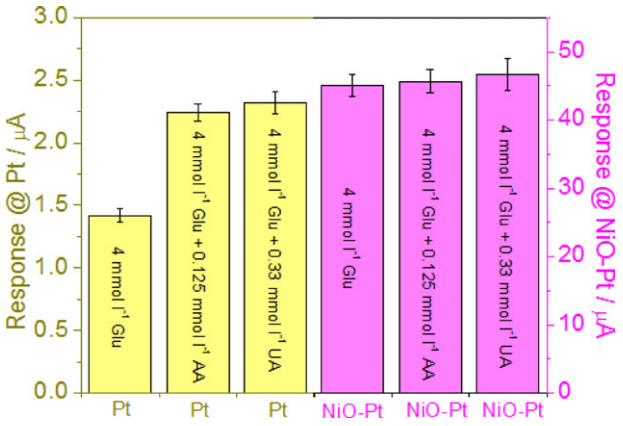

Fig. 8. Current responses obtained at Pt NFs/GCE and NiO–Pt NFs/GCE towards 4 mM glucose, 4 mM glucose with 0.125 mM AA, and 4 mM glucose with 0.33 mM UA in 0.1 M NaOH solution with a stirring rate of 300 rpm at an applied potential of +0.6 V.

that the charge-exclusion property of Nafion is not the major factor to minimize the interference in our non-enzymatic glucose detection at +0.6 V vs. Ag/AgCl (3 M KCl). The excellent selectivity of the hybrid nanofibers may be attributed to the enhanced oxidation of glucose as well as the repelling effect of the negative surface of NiO towards the negatively charged AA and UA in alkaline electrolyte [15].

The inter-electrode reproducibility of the NiO–Pt nanofibers based sensor was further evaluated using 6 electrodes, which were prepared following the same protocol. A small relative standard deviation (R.S.D.) of 7.4% in the detections of 200 μM glucose at +0.6 V demonstrated that the preparation method was highly reproducible. 8 successive measurements of 200 μM glucose at one NiO–Pt NFs/GCE yielded a R.S.D. of 6.7%, indicating excellent intra-electrode reproducibility and stability under continuous detection.

4. Conclusions

We have successfully fabricated NiO–Pt nanofibers using a two-step method. Pt is dispersed as tiny dots along a NiO matrix. The effect of Pt in glucose sensing was illustrated by a comparison study between NiO–Pt, NiO and Pt nanofibers. Results showed that the presence of Pt nanoparticles in NiO–Pt nanofibers could greatly improve the sensitivity of glucose detection at +0.6 V. Excellent selectivity and reproducibility were also demonstrated. These features indicate that the NiO–Pt hybrid nanofiber is a novel and promising candidate for nonenzymatic glucose sensors.

Acknowledgements

We greatly appreciate the funding from NSF and DOE. Y.D. also acknowledges the supports from the UConn CESE through the Graduate Student Research Assistantship Program in Support of Multidisciplinary Environmental Activities by Faculty Members.

Appendix A. Supplementary data

Supplementary data associated with this article can be found, in the online version, at doi:10.1016/j.electacta.2011.09.039.

References

[1] L.Q. Rong, C. Yang, Q.Y. Qian, X.H. Xia, Talanta 72 (2007) 819.
[2] X.J. Bo, J.C. Ndamanisha, J. Bai, L.P. Guo, Talanta 82 (2010) 85.
[3] W. Wang, L. Zhang, S. Tong, X. Li, W. Song, Biosens. Bioelectron. 25 (2009) 708.
[4] S. Park, T.D. Chung, H.C. Kim, Anal. Chem. 75 (2003) 3046.
[5] J.H. Yuan, K. Wang, X.H. Xia, Adv. Funct. Mater. 15 (2005) 803.
[6] Y.Y. Song, D. Zhang, W. Gao, X.H. Xia, Chem. Eur. J. 11 (2005) 2177.
[7] J. Wang, D.F. Thomas, A. Chen, Anal. Chem. 80 (2008) 997.
[8] H.F. Cui, J.S. Ye, W.D. Zhang, C.M. Li, J.H.T. Luong, F.S. Sheu, Anal. Chim. Acta 594 (2007) 175.
[9] X. Zhang, K.Y. Chan, A.C.C. Tseung, J. Electroanal. Chem. 386 (1995) 241.
[10] D. Li, Y.N. Xia, Nano Lett. 3 (2003) 555.
[11] H. Wu, D.D. Lin, W. Pan, Appl. Phys. Lett. 89 (2006) 3.
[12] X.H. Yang, C.L. Shao, H.Y. Guan, X.L. Li, H. Gong, Inorg. Chem. Commun. 7 (2004) 176.
[13] H.Y. Guan, C.L. Shao, S.B. Wen, B. Chen, J. Gong, X.H. Yang, Mater. Chem. Phys. 82 (2003) 1002.
[14] Y. Ding, Y. Wang, L. Su, M. Bellagamba, H. Zhang, Y. Lei, Biosens. Bioelectron. 26 (2010) 542.
[15] Y. Ding, Y. Wang, L. Su, H. Zhang, Y. Lei, J. Mater. Chem. 20 (2010) 9918.
[16] W. Nuansing, S. Ninmuang, W. Jarernboon, S. Maensiri, S. Seraphin, Mater. Sci. Eng. B: Solid State Mater. Adv. Technol. 131 (2006) 147.
[17] N.A.M. Barakat, K.D. Woo, M.A. Kanjwal, K.E. Choi, M.S. Khil, H.Y. Kim, Langmuir 24 (2008) 11982.
[18] V.G. Pol, E. Koren, A. Zaban, Chem. Mater. 20 (2008) 3055.
[19] J.L. Shui, J.C.M. Li, Nano Lett. 9 (2009) 1307.
[20] Z.Y. Hou, P.P. Yang, C.X. Li, L.L. Wang, H.Z. Lian, Z.W. Quan, J. Lin, Chem. Mater. 20 (2008) 6686.
[21] D. Li, J.T. McCann, Y.N. Xia, J. Am. Ceram. Soc. 89 (2006) 1861.
[22] S. Park, H. Boo, T.D. Chung, Anal. Chim. Acta 556 (2006) 46.
[23] B. Beden, F. Largeaud, K.B. Kokoh, C. Lamy, Electrochim. Acta 41 (1996) 701.
[24] L.M. Lu, L. Zhang, F.L. Qu, H.X. Lu, X.B. Zhang, Z.S. Wu, S.Y. Huan, Q.A. Wang, G.L. Shen, R.Q. Yu, Biosens. Bioelectron. 25 (2009) 218.
[25] E. Reitz, W.Z. Jia, M. Gentile, Y. Wang, Y. Lei, Electroanalysis 20 (2008) 2482.
[26] L.C. Jiang, W.D. Zhang, Biosens. Bioelectron. 25 (2010) 1402.
[27] L. Ozcan, Y. Sahin, H. Turk, Biosens. Bioelectron. 24 (2008) 512.
[28] A. Safavi, N. Maleki, E. Farjami, Biosens. Bioelectron. 24 (2009) 1655.
[29] J.S. Ye, Y. Wen, W.D. Zhang, L.M. Gan, G.Q. Xu, F.S. Sheu, Electrochem. Commun. 6 (2004) 66.
[30] S. Hrapovic, J.H.T. Luong, Anal. Chem. 75 (2003) 3308.